Indian Journal of Fibre& Textile Research
Vol. 50, March 2025, pp. 53-61
DOI: 10.56042/ijftr.v50i1.5114

Thermal and morphological properties of alkali-treated *Alstonia macrophylla* fibres

Vinu Kumar S M[1,a], Sakthivelmurugan E[2] & Harwinder Singh[3]

[1]Department of Mechanical Engineering, Sri Krishna College of Technology, Kovaipudur, Coimbatore 641 042, India

[2]Department of Mechanical Engineering, Bannari Amman Institute of Technology, Sathyamangalam, Erode 638 401, India

[3]Department of Textile Engineering, Panipat Institute of Engineering & Technology, Panipat 132 102, India

Received 24 August 2023; revised received and accepted 25 April 2024

This study examines the thermal, wettability, and surface properties of the untreated and alkali-treated *Alstonia macrophylla* (ASM) fibres extracted from the seed pods. Alkali treatment leads to an increase in cellulose content, enhancing the fibre's thermal stability, crystallinity, and surface roughness. Dynamic contact angle measurements indicate improved wettability of treated ASM fibres, confirming their superior interaction in liquid-phase environments. Field emission scanning electron microscopy and Atomic Force Microscopy analyses reveal a significant increase in surface roughness in treated fibres compared to untreated ones.

Keywords: Alkali treatment, *Alstonia macrophylla* fibre from seed pods, Surface roughness, Thermal stability, Wettability

1 Introduction

In the last three decades, the global community has become increasingly aware of the adverse environmental consequences of the widespread utilisation of synthetic or artificially created fibres like glass, carbon, and Kevlar in polymer composites[1-4]. This growing recognition has spurred researchers and scholars to explore and develop novel, sustainable, and environmentally friendly materials for reinforcement in polymer matrix composites. Therefore, natural fibres have emerged as a promising alternative due to their abundance and advantageous properties like non-toxicity, low cost, lightness, biodegradability, recyclability and good thermal and specific properties[5-10]. These attributes have increased adoption in furniture, automotive, electronic, packaging, construction, and airplane industries[11,12]. Moreover, low greenhouse gas emissions, good mechanical attributes, and minimal energy expenditure during production have positioned natural fibres as promising contenders to their synthetic counterparts. Their increased use in the industry has been particularly pronounced over the last twenty years, underlining their feasibility and potential as sustainable alternatives[13,14].

Despite their advantages, natural fibres exhibit certain limitations, which can be addressed through surface modification techniques. Variability in fibre properties is frequently observed among different parts of the same plant, such as stems, leaves, seed pods, roots and fruits[15]. In addition, weathering, soil condition, plant growth, and methods of fibre extractions significantly influence properties such as thermal stability, mechanical, crystallinity, surface roughness, and chemical composition of the extracted fibres[16-18]. Any changes in these properties can affect the performance of the final polymer composite materials.

Extensive research has been conducted on fibres extracted from roots[18-20], stem[21] leaves[15,22]and fruits[23,24] to identify their potential use as reinforcing agents in polymer matrix composites. However, limited studies exist on fibres derived from seed pods, presenting an opportunity for further exploration in composite applications. Longer fibres can be extracted from the dry seed pods of the plant *Alstonia macrophylla* by retting process. It has been reported that longer fibres offer superior properties in developing lightweight composite materials compared to short fibres[23]. In our previous investigation[24], tensile strength, crystallinity, chemical composition, and fibre length distribution of the *A. macrophylla* fibre were reported successfully. However, other crucial fibre

[a]Corresponding author.
E-mail: vinukmr1988@gmail.com

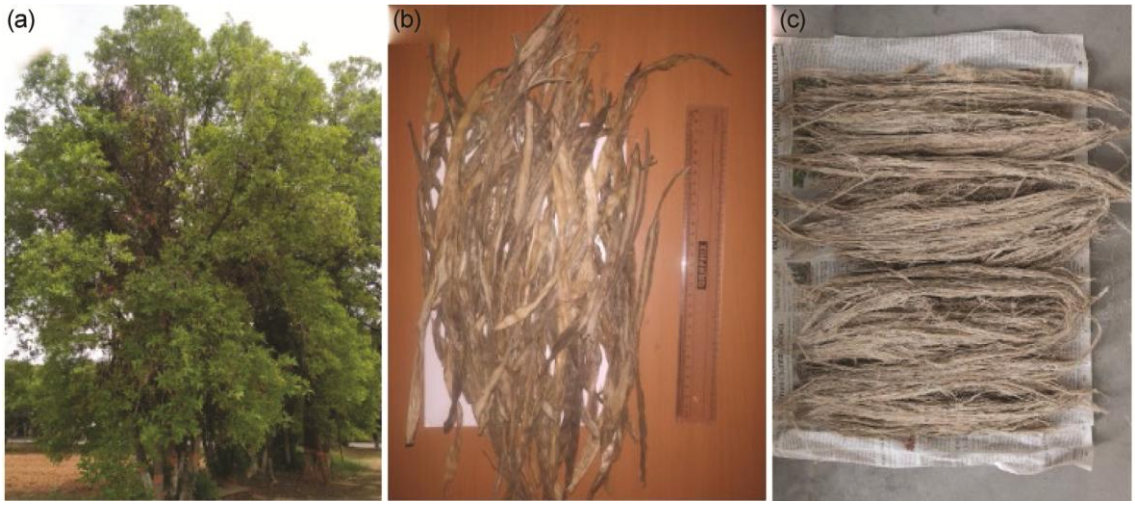

Fig. 1 — Morphology of *A. macrophylla* (a) tree, (b) dry seedpods, and (c) extracted fibres

properties, such as thermal stability, chemical structure and surface morphology, require further investigation to assess their suitability for composite applications. Therefore, in this study, Thermogravimetric Analysis (TGA), Nuclear Magnetic Resonance (NMR), Atomic Force Microscopy (AFM), and Field Emission Scanning Electron Microscopy (FESEM) techniques are employed to characterise these fibres comprehensively.

2 Materials and Methods

2.1 Raw Material

Alstonia macrophylla (ASM) is a tree native to Asia and predominantly used for medical purposes in Tamil Nadu, India. In this study, cellulosic fibres were extracted from the dry seed pods of the tree.

2.2 Fibre Extraction

Dry seed pods were collected, cleaned with water to remove any debris, and subsequently soaked in water for approximately two weeks to allow for the removal of the hard skin through retting[25,26]. This biological degradation helped remove the hard outer skin, allowing for the manual extraction of fibres, which were then thoroughly cleaned with running water. The extracted fibres were dried in sunlight at room temperature of 28 ºC. The ASM tree, dry seed pods, and extracted fibres are depicted in Fig. 1. The tensile strength and Young's modulus of the ASM fibre are 239.45 +12.89 MPa and 2.09 GPa, respectively[24]. The chemical composition of ASM fibre consists of 72.59% cellulose, 28.95% hemicellulose, 12.78% lignin, 3.62% wax, 8.14% moisture, and 1.28% ash.

2.2.1 Alkali Treatment of ASM Fibre

Sodium hydroxide (98% purity) and acetic acid (98% purity) were procured from Sigma Aldrich Pvt Ltd, India. The fibres were cleaned and dried before being soaked in a 5% aqueous solution of NaOH for 60 min at 22 °C. After that, they were washed with a 1% acetic acid solution to eliminate any remaining traces of NaOH. The fibres were then oven-dried at 65 °C for 120 min. Finally, both untreated and treated fibres were analysed for comparative studies.

2.3 CP/MAS ^{13}C-NMR Spectroscopy

Cross-polarisation/magic-angle spinning (CP/MAS) ^{13}C-NMR spectroscopy was performed to examine the structural changes in untreated and alkali-treated fibre samples using a JEOL ECX 400 MHz spectrometer[29]. Fibre samples (350–400 mg) were ground into a fine powder and placed in a 4 mm rotor, which was spun at 10 kHz, at 28 ºC with a constant operating frequency of 100 MHz.

2.4 Thermogravimetric Analysis (TGA)

TGA was performed in the thermal analyser, NETZSCH STA 2500 (Regulus, Germany), to understand the thermal stability of untreated and alkali-treated ASM fibres. Samples were heated from 28 °C to 550 °C at a controlled heating rate of 10 °C/min in a nitrogen atmosphere supplied at a flow rate of 60 mL/min. The kinetic activation energy (E_a) of the fibres was determined from the slope of Broido's graph, which was plotted in

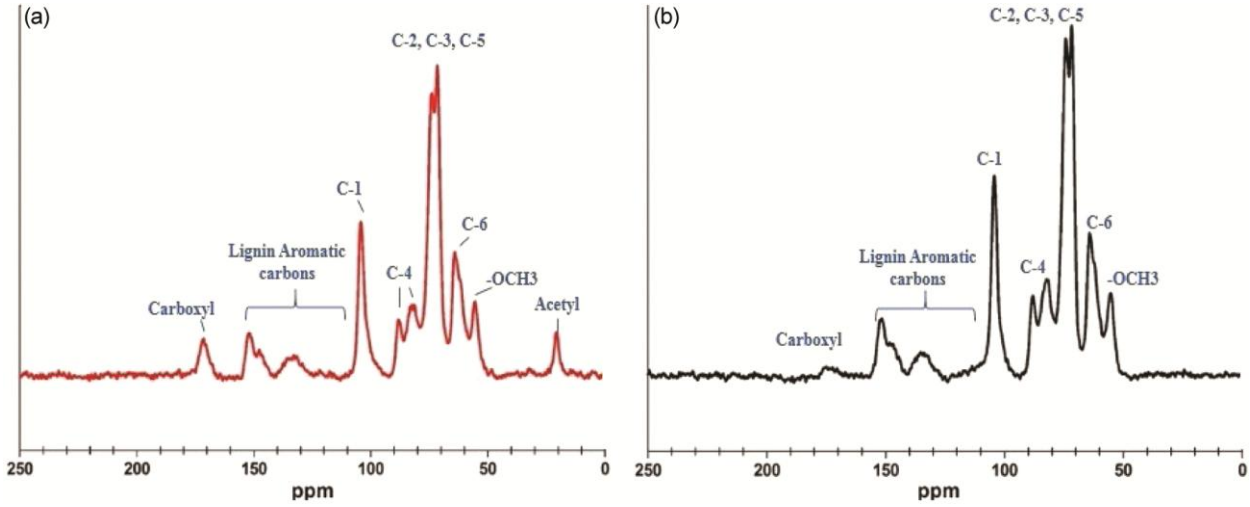

Fig. 2 — Solid-state NMR spectra of (a) untreated and (b) alkali-treated fibres

accordance with Eq. (1) by considering the normalised weight against the inverse of temperature[20,30]. E_a was calculated to find the authenticity of the ASM fibre as a suitable reinforcement in polymer composites[20].

$$\ln\left[\ln\left[\frac{1}{y}\right]\right] = -\frac{E_a}{R}\left(\frac{1}{T}\right) + K \quad \ldots (1)$$

where y is normalized weight (w_t/w_i); w_t, weight of the fibre sample at any given time; w_i, initial weight of the fibre sample; E_a, activation energy (kJ/mole); T, temperature (Kelvin); R, universal gas constant (8.314 J/kg/mol); and K, the reaction rate constant.

2.5 Dynamic Contact Angle Measurement

Contact angle measurements were carried out to determine the wettability properties of the materials. Two methods are widely followed to determine the contact angles: the static drop method and the dynamic method[31]. This study employed the latter technique using a Force Tensiometer K100 (Kruss, Germany). Fibres of suitable length (50 mm) were dipped into a water medium to assess the dynamic process of wetting.

2.6 FESEM Analysis

The surface morphology of untreated and alkali-treated ASM fibres was examined using FESEM (Carl Zeiss Sigma-300, Schottky FEG). Both longitudinal and cross-sectional images of the fibres were captured at various magnifications.

2.7 AFM Analysis

Surface roughness characteristics of the fibres were evaluated using AFM (Easyscan 2, Nanosurf-Switzerland). Parameters such as average roughness and root mean square roughness were investigated to assess surface modifications[32].

3 Results and Discussion

3.1 CP/MAS ^{13}C-NMR Spectroscopy

Figure 2 (a) and 2 (b) shows the CP/MAS ^{13}C-NMR spectra for untreated and alkali-treated fibres respectively. The spectra exhibit an intense peak at 171.48-175 ppm due to the presence of hemicellulose units, mainly from CH_3COO and COOH groups. A similar peak at 147.64-152.23 ppm confirms the presence of lignin, corresponding to aromatic carbons[33]. Additionally, a broad peak of lesser intensity in the region 132.89-35.33 ppm further confirms the lignin fractions. A sharp and intense signal at 104.27 ppm corresponds to the C1 carbons of cellulose and hemicellulose units[34].Among the carbons in cellulose molecules, C2, C3, and C5 appear in the 71.64-74.28 ppm range, whereas C4 and C6 are observed at 88.05 ppm and 67.33 ppm, respectively. The peaks between 71-75 ppm, exhibiting the highest intensity, are associated with hemicellulose units. The signals at 82.38 ppm and 88.05 ppm further indicate the presence of hemicellulose, while the peak at 55.42 ppm is related to OCH_3 carbons of lignin. A sharp peak with moderate intensity at 20.74 ppm, mainly for untreated fibres, indicates the presence of CH_3COO groups characteristic of hemicellulose [29,33].

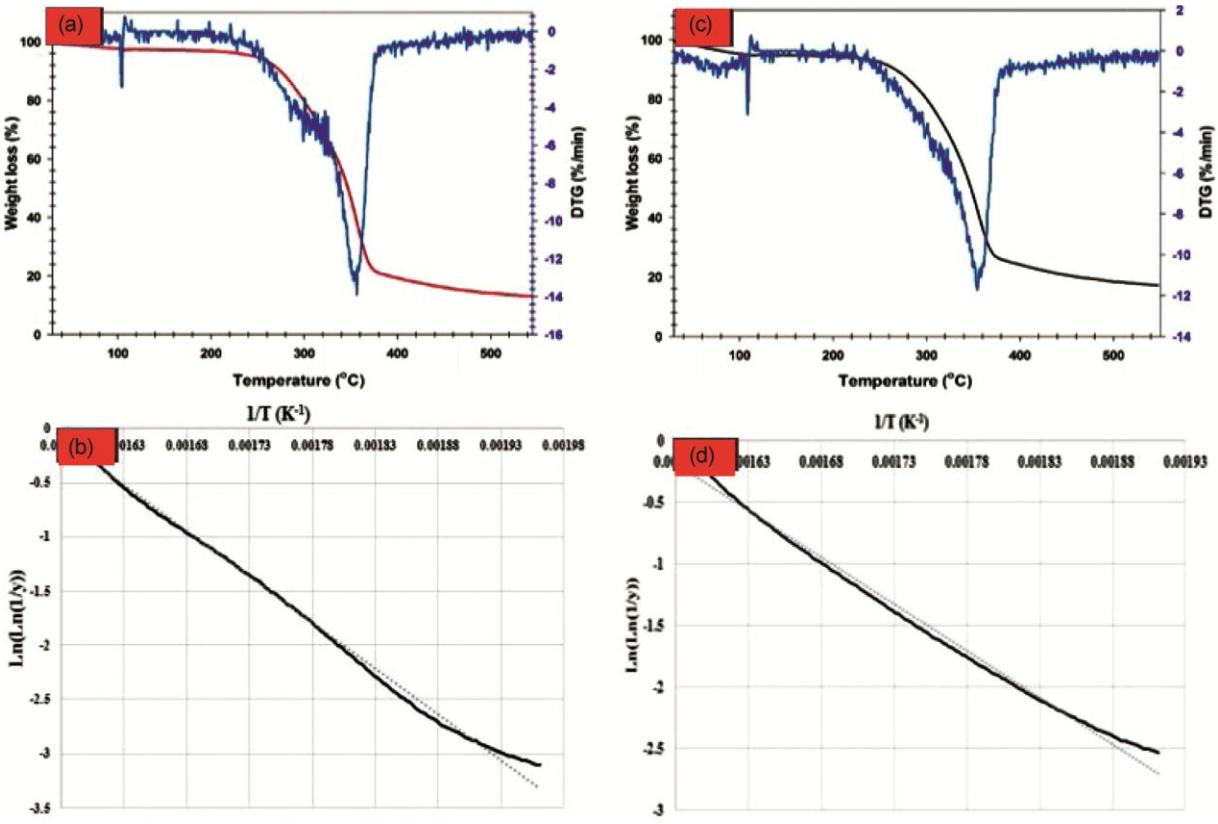

Fig. 3 — TGA/DTG and Broidos plots of (a, b) untreated and (c, d) alkali-treated fibres

The NMR spectra of alkali-treated fibres [Fig. 2 (b)] reveal notable characteristics. In the region spanning 171-175 ppm, there is a notable decrease in the intensity of the carbonyl peak, accompanied by a subsequent increase in intensity at 151.65 ppm, appearing as a shoulder to the 147.64 ppm signal. Furthermore, a significant observation emerges from the disappearance of the signal at 20.74 ppm, indicating the removal of hemicellulose content from the surface of the treated ASM fibre. Signals within the range of 55 ppm to 110 ppm remain unchanged, suggesting stability in these regions. These findings suggest that the alkali treatment has a notable impact on hemicellulose units, potentially leaving other components, such as cellulose and lignin, relatively undisturbed. This observation is consistent with FTIR and chemical analyses from our earlier investigation[24].

3.2 Thermogravimetric Analysis

The thermal properties of untreated and alkali-treated fibres are analysed through TG/DTG curves, as presented in Fig. 3. Understanding the thermal behaviour of cellulosic fibres is imperative for evaluating their applicability across different domains. Both untreated and treated fibres exhibit an initial mass degradation of approximately 5%, which occurs from 28 °C to 251.07 °C in untreated fibres and up to 126.5 °C in treated fibres. This initial degradation likely results from the evaporation of water molecules due to the hydrophilic nature of fibres[26]. In the subsequent phase, another 5% mass degradation is recorded, occurring between 251.07 °C-273 °C for untreated fibres and 126.5 °C-265 °C for treated fibres. This stage of degradation can be attributed to the breakdown of amorphous content and cellulose linkages within the fibres[20,27].

At this stage, a cumulative loss of 10% mass degradation is observed for both fibres. The major thermal degradation phase, associated with cellulose and hemicellulose decomposition, occurs at 274-376 °C for untreated fibres and 269-372 °C for treated fibres, resulting in mass losses of 79.23% and 73.45%, respectively. These findings indicate that alkali treatment enhances thermal stability. Furthermore, at 550 °C, char residue percentages of 13.36% and 18.28% are noted for untreated and treated fibres, respectively. The higher char residue observed in treated ASM fibres can be attributed to a

Table 1 — Comparison of the thermal stability of the ASM fibre with other natural fibres[18]

Fibre source	Thermal stability (°C)	Max. thermal degradation (°C)	Kinetic activation energy (kJ/mol)	References
Lygeum spartum L.	220	338	68.77	7
Cissus quadrangularis stem	270	342.1	74.18	11
Common reed	230	370	-	19
Ficus religiosa	325	400	68.02	21
Piliostigma racemosa	244	327	67.91	22
Heteropogon contortus	220	337.7	-	23
Shwetark	225	350	-	24
Acacia nilotica L.	210	339	69.73	25
Sansevieria ehrenbergii	223	232	-	26
Prosopis juliflora bark	217	331	76.72	27
Juncus effuses L	200	300	-	28
Napier grass strands	220	383	-	29
Phaseolus vulgaris	250	328	-	30
Catharanthus roseus	203	296	-	31
Cereus hildmannianus	285	356.7	-	32
Untreated ASM fibre	274	373	62.79	Present work
Alkali-treated ASM fibre	269	375	73.48	Present work

notable enhancement in the cellulose percentage ratio[27]. A comparison of the thermal properties of ASM fibres with those of other natural fibres is shown in Table 1.

The kinetic activation energy (Ea), representing the minimum energy required for fibre degradation, is determined from Broido's plot (Fig. 3). The activation energies for untreated and treated fibres are 62.79 kJ/mol and 73.48 kJ/mol, respectively, indicating a 17% increase after the alkali treatment. This is likely attributed to the removal of hemicellulose and other wax contaminants[35]. The thermal stability comparison of ASM fibres with other natural fibres is summarised in Table 1, demonstrating their suitability for polymer composite reinforcement at processing temperatures below 320 °C[35].

3.3 Dynamic Contact Angle Measurement

Figure 4 illustrates the variation in dynamic contact angle with immersion depth for untreated and alkali-treated fibres. The contact angle for untreated fibres is 109.22°, whereas for treated fibres, it is reduced to 88.95°. This decrease is attributed to the removal of non-polar components such as wax and lignin. Removal of these contaminants affects the surface roughness properties and, consequently, the hysteresis of the contact angle[36]. The advancing and receding contact angles of treated fibres are consistently lower than those of untreated fibres, indicating an increase in surface polarity, as corroborated by FTIR and chemical analysis[24]. These findings are consistent with the existing literature[37,38].

3.4 FESEM Analysis

FESEM analysis is conducted to elucidate the surface morphology of untreated and alkali-treated fibres, providing insights into their interfacial adhesion between the fibres and matrix[39]. Fig. 5 presents a longitudinal view of the raw ASM fibre surface, revealing impurities, voids and waxy substances. The surface of the raw ASM fibre exhibits cavities and pits [Fig. 5 (a)] similar to observations for other plant fibres such as *Juncus effuses*, *Coccinia grandis* and *Strelitzia reginae*. The presence of cavities can lead to a reduction in the mechanical properties of the fibre. Fig. 5(b) displays a higher magnification image of the ASM fibre, revealing a structure composed of various cellulosic fibrils held together by lignin and hemicellulose. Additionally, the irregular surface of the ASM fibre is attributed to the presence of hemicellulose, lignin residues, and other wax substances. These contaminants have the potential to weaken the fibre and matrix adhesion.

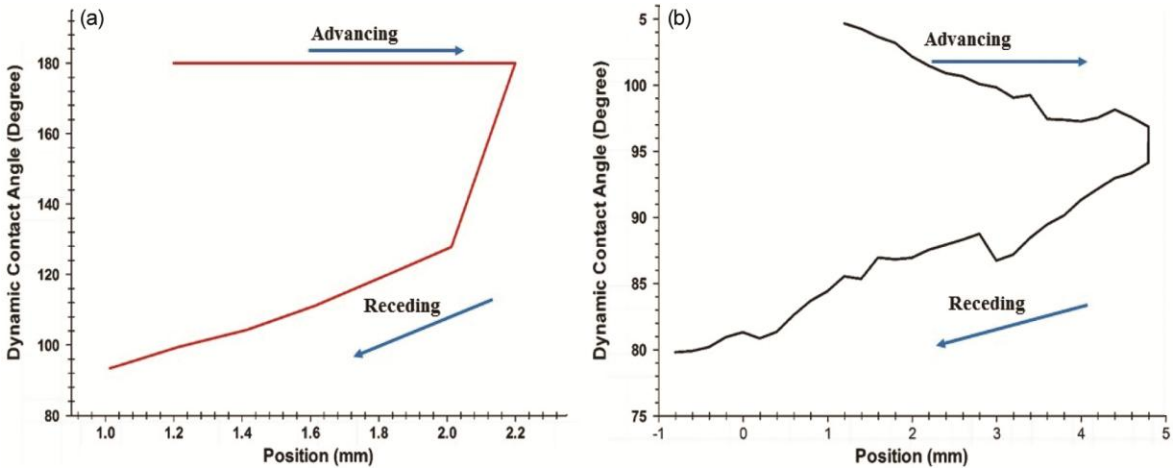

Fig. 4 —Advancing and receding contact angles of (a) untreated and (b) alkali-treated fibres

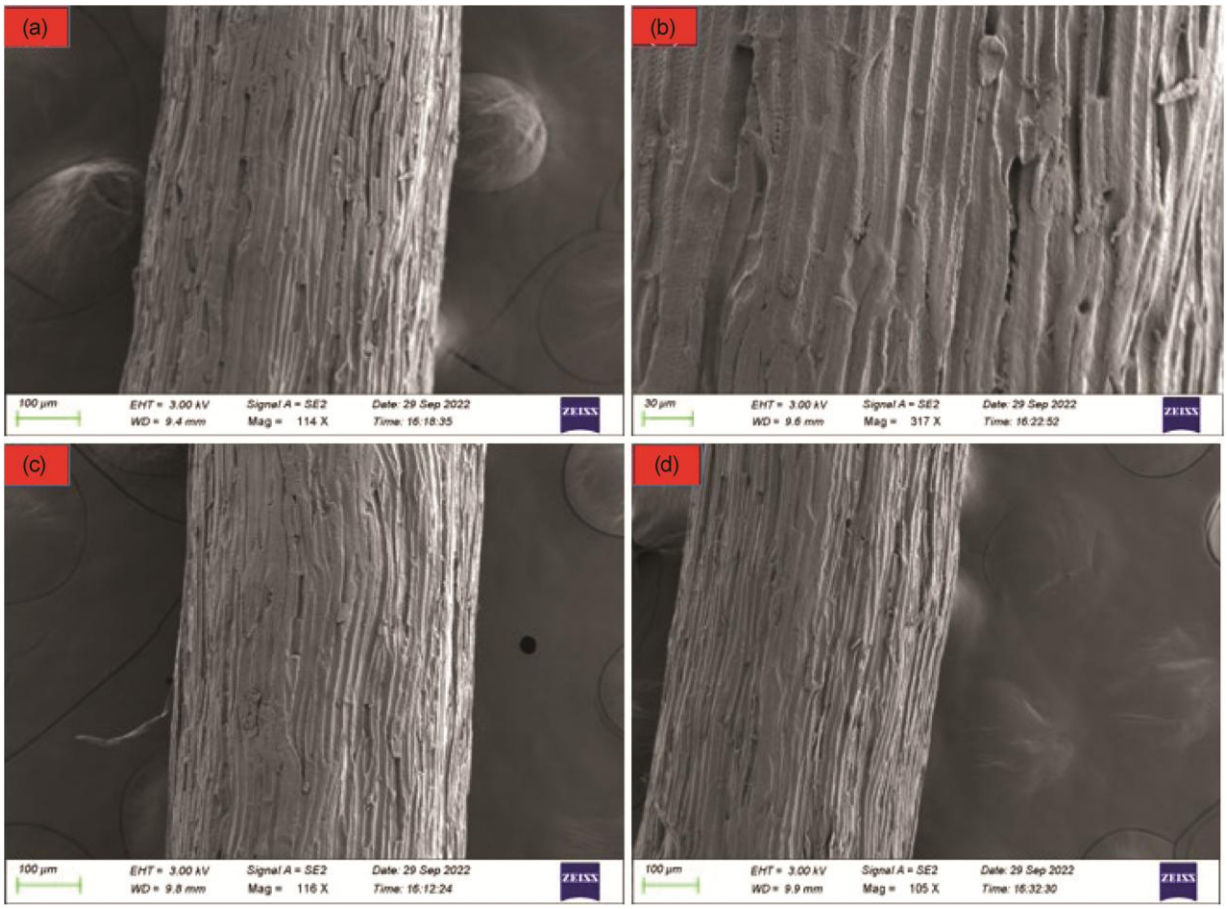

Fig. 5 — FESEM images of (a, b) untreated and (c, d) alkali-treated fibres

Therefore, alkali treatment of the fibres is essential as it eliminates impurities from the fibre surfaces. The surface of alkali-treated fibres [Fig. 5 (c and d)] appears significantly smoother due to the removal of hemicellulose, lignin residues, and waxy contaminants. Alkali treatment introduces functional groups that enhance bonding in polymer composites and contribute to a decrease in fibre diameter[40]. These observations confirm the potential of alkali-treated ASM fibres as reinforcement materials for lightweight composite applications.

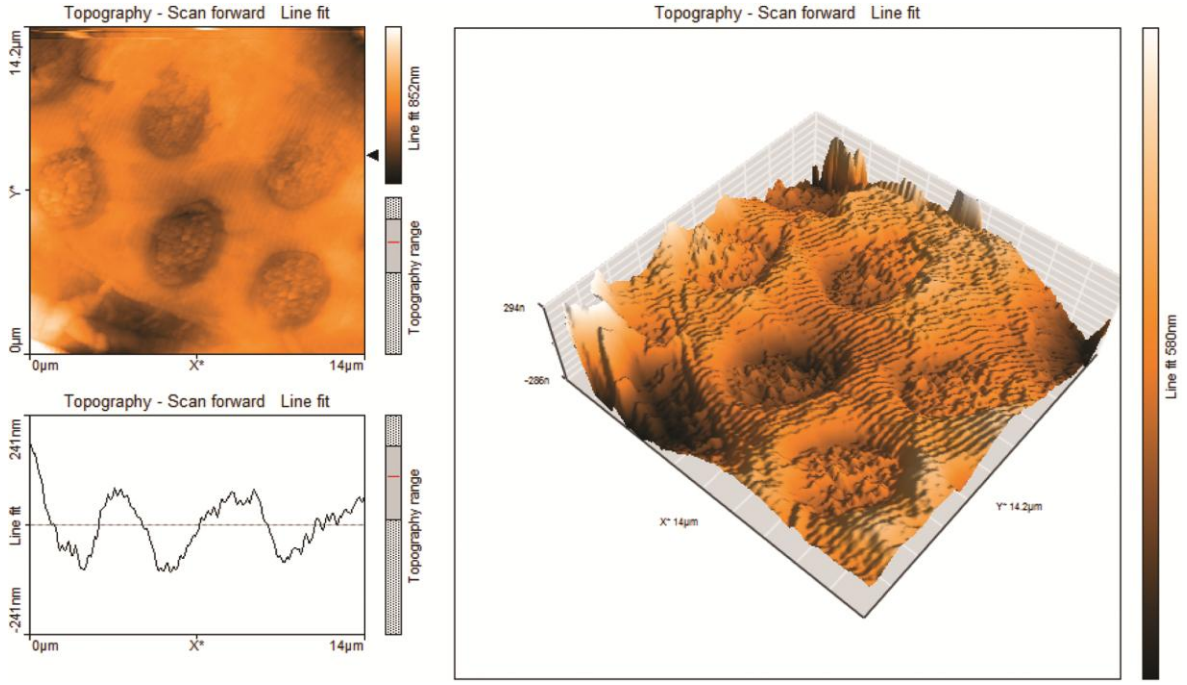

Fig. 6 — AFM images of untreated ASM fibre

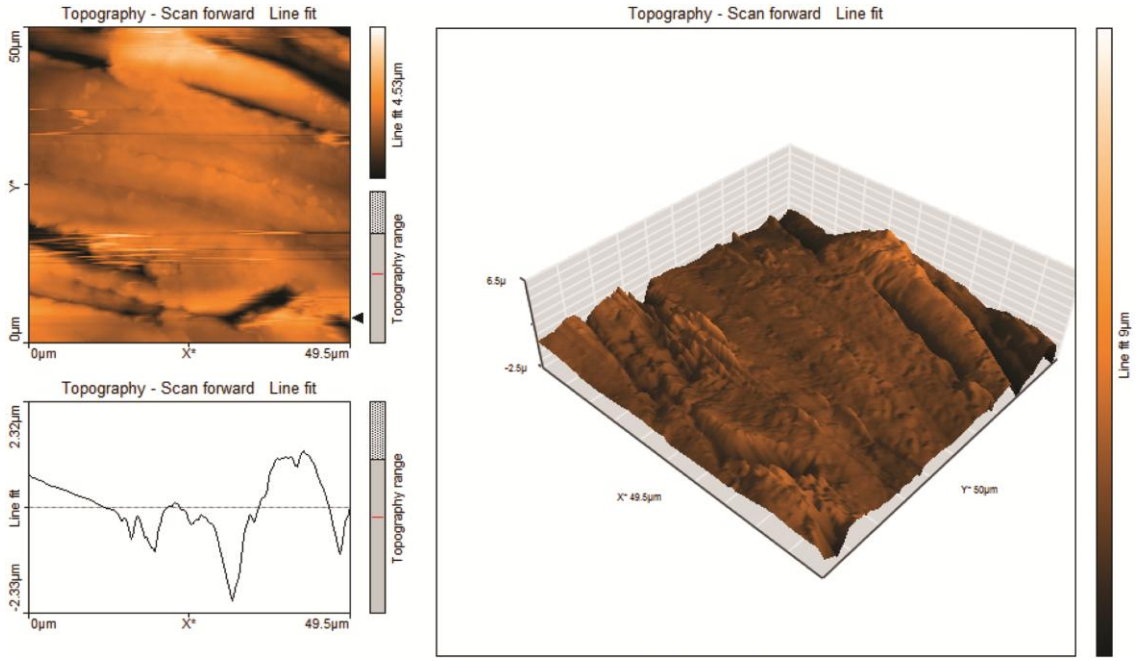

Fig. 7 — AFM images of alkali-treated ASM fibre

3.5 Atomic Force Microscopy

The surface topography of untreated and alkali-treated fibres is studied using AFM images obtained in 2D and 3D scales. Figure 6 clearly illustrates that the untreated fibre possesses a higher quantity of surface pores, a finding corroborated by FESEM analysis. Comparatively, the average surface roughness (Ra) and root-mean-square roughness (Rq) of untreated fibres are notably elevated, measuring at 93.41 nm and 119.91 nm, respectively. These values surpass those observed in other cellulosic fibres from *Phaseolus vulgaris*, *Carica papaya*, *Ficus religiosa*, banana peduncle, *Piliostigma racemosa*, and Shwetark. Figure 7 indicates a notable reduction in

surface pores of the fibres following chemical treatment. The average surface roughness (Ra) and root-mean-square roughness (Rq) of the chemically treated fibres measure at 235.28 nm and 305.5 nm, respectively. These values notably exceed those of untreated fibres, suggesting the effective removal of hemicellulose, lignin, wax, and other impurities from the fibres' surface. This process is detailed in reference[29].

Conclusion

The present study investigates the structural, thermal, and surface characteristics of untreated and alkali-treated *A. macrophylla* fibres to assess their suitability as reinforcement in polymer composites. CP/MAS ^{13}C-NMR spectroscopy confirms the removal of hemicellulose following alkali treatment. TGA reveals that alkali-treated fibres exhibit improved thermal stability, with a higher char residue of 18.28% compared to 13.36% in untreated fibres. The kinetic activation energy increases after alkali treatment from 62.79 kJ/mol to 73.48 kJ/mol. Furthermore, the alkali-treated fibre demonstrates superior wettability compared to the untreated fibres, as evidenced by dynamic contact angle measurements. FESEM analysis confirms that alkali treatment smooths the fibre surface by eliminating impurities, while AFM analysis reveals a reduction in surface pores and an increase in roughness parameters. It demonstrates that alkali-treated ASM fibres exhibit enhanced thermal stability, improved wettability, and superior surface characteristics, making them promising candidates for lightweight and high-performance composite applications.

References

1 Pradhan R, Palai B K, Thatoi D N, Elayaperumal A & Nalla J S, *Biomass Convers Biorefin*, 15 (5) (2025) 7947, https://doi.org/10.1007/s13399-024-05690-3.

2 Ramakrishnan S K, Arivendan A & Vijayananth K, *Int J Biol Macromol*, 285 (2025) 138102, doi: https://doi.org/10.1016/j.ijbiomac.2024.138102.

3 Vinu kumar S M, Jeyakumar R & Sakthivelmurugan E, *Cell Chem Technol*, 58 (5) (2024) 547, doi: https://doi.org/10.35812/CelluloseChemTechnol.2024.58.51.

4 Skosana S J, Khoathane C & Malwela T, *J Thermoplast Compos Mater*, 38 (2) (2025) 754, doi: https://doi.org/10.1177/08927057241254324.

5 Vivas E A, Castillo H S V & Acosta E G, *J Nat Fibers*, 22 (1) (2025) 2453489, doi: https://doi.org/10.1080/15440478.2025.2453489.

6 Birlie B & Mamay T, *Int J BiolMacromol*, 271 (2024) 132858, doi: https://doi.org/10.1016/j.ijbiomac.2024.132858.

7 Kumar S V & Singh H, *Ind J Fibre Text*, 48 (3) (2023) 326, doi: https://doi.org/10.56042/ijftr.v48i3.6057.

8 Jeyakumar R, Vinu Kumar S M, Rishi J P & Sasikumar C, *Mater Res*, 27 (2024) e20230543, doi: https://doi.org/10.1590/1980-5373-MR-2023-0543.

9 Sakthivelmurugan E, Senthilkumar G & Kumar S V, *Mater Res*, 26 (2023) e20230108, doi: https://doi.org/10.1590/1980-5373-MR-2023-0108.

10 Sakthivelmurugan E, Senthil K G, Vinu K S M & Singh H, *J BrazSoc*, 45 (8) (2023) 400, doi: https://doi.org/10.1007/s40430-023-04339-y.

11 Rajiev R, Kumar S V, Singh H & Sakthivelmurugan E, *Ind J Fibre Text*, 48 (4) (2023) 396, doi: https://doi.org/10.56042/ijftr.v48i4.7640.

12 Shettahalli M V K, Kallippatti L S K & Kaliappagounder S, *J Nat Fibers*,19 (15) (2022) 10367,doi: https://doi.org/10.1080/15440478.2021.1993504.

13 Karimah A, Ridho M R, Munawar S S, Ismadi, Amin Y, Damayanti R, Lubis M A R, Wulandari A P, Nurindah & Iswanto A H, *Polymers*, 13 (24) (2021) 4280, doi: https://doi.org/10.3390/polym13244280.

14 Lemita N, Deghboudj S, Rokbi M, Rekbi F M L & Halimi R, *J Compos Mater*, 56 (1) (2022) 99, doi: https://doi.org/10.1177/00219983211049285.

15 Mansour R, Abdelaziz A & Fatima Z A, *Res J Text Appar*, 22 (3) (2018) 195, doi: https://doi.org/10.1108/RJTA-02-2018-0009.

16 Makri H, Rokbi M, Meddah M, Belayachi N & Khaldoune A, *J Compos Mater*, (2023), doi: https://doi.org/10.1177/00219983231184020.

17 Gedik G, *Cellulose*, 28 (2021) 6899, doi: https://doi.org/10.1007/s10570-021-03952-1.

18 Maheshwaran M, Hyness N, Senthamaraikannan P, Saravanakumar S & Sanjay M, *J Nat Fibers*, 15 (2018) 789, doi: https://doi.org/10.1080/15440478.2017.1364205.

19 Indran S, Raj R E & Sreenivasan V, *Carbohydr Polym*, 110 (2014) 423, doi: https://doi.org/10.1016/j.carbpol.2014.04.051.

20 Moshi A A M, Ravindran D, Bharathi S S, Indran S, Saravanakumar S & Liu Y, *Int J Biol Macromol*, 142 (2020) 212, doi: https://doi.org/10.1016/j.ijbiomac.2019.09.094.

21 Kılın Ç A Ç, Köktaş S, Atagür M & Seydibeyoglu M Ö, *J Nat Fibers*, 15 (3) (2018) 325, doi: https://doi.org/10.1080/15440478.2017.1325813.

22 Bezazi A, Belaadi A, Bourchak M, Scarpa F & Boba K, *Compos Part B Eng*, 66 (2014) 194, doi: https://doi.org/10.1016/j.compositesb.2014.05.014.

23 Bhatnagar A & Sain M, *J Reinf Plast Comp*, 24 (12) (2005) 1259, doi: https://doi.org/10.1177/0731684405049864.

24 Sakthivelmurugan E, Senthilkumar G, Kumar S & Singh H, *Cellul Chem Technol*, 55 (2023) 39908, doi: https://doi.org/10.35812/CelluloseChemTechnol.2023.57.35.

25 Kulandaivel N, Muralikannan R & KalyanaSundaram S, *J Nat Fibers*, 17 (5) (2018) 769, doi: https://doi.org/10.1080/15440478.2018.1534184.

26 Pandiarajan P & Kathiresan M, *Int J Polym Anal Charact*, 23 (5) (2018) 442, doi: https://doi.org/10.1080/ 1023666X.2018.1474327.

27 Vinod A, Vijay R, Lenin S D, Khan A, Sanjay M, Siengchin S, Verpoort F, Alamry K A & Asiri A M, *J Ind Text*, 51 (2022) 2444S, doi: https://doi.org/10.1177/ 1528083 720942614.

28 Arthanarieswaran V, Kumaravel A & Saravanakumar S, *Int J Polym Anal Charact*, 20 (8) (2015) 704, doi: https://doi.org/10.1080/1023666X.2015.1081133.
29 Ravindran D, Bharathi S R S & Indran S, *Int J Biol Macromol*, 156 (2020) 997, doi: https://doi.org/10.1016/j.ijbiomac.2020.04.117.
30 Ramkumar R & Saravanan P, *J Nat Fibers*, 19 (13) (2022) 5101, doi: https://doi.org/10.1080/15440478.2021.1875356.
31 Carroll B, *J Colloid Interface Sci*, 57 (3) (1976) 488, doi: https://doi.org/10.1016/0021-9797(76)90227-7.
32 Pitchayya P G, Manimaran P & Vignesh V, *J Nat Fibers*, 18 (12) (2021) 2102, doi: https://doi.org/10.1080/15440478.2020.1723777.
33 Reddy K O, Guduri B & Rajulu A V, *J Appl Polym Sci*, 114 (1) (2009) 603, doi: https://doi.org/10.1002/app.30584.
34 Fort D A, Remsing R C, Swatloski R P, Moyna P, Moyna G & Rogers R D, *Green Chem*, 9 (1) (2007) 63, doi: https://doi.org/10.1039/b607614a.
35 Senthamaraikannan P & Kathiresan M, *Carbohydr Polym*, 186 (2018) 332, doi: https://doi.org/10.1016/ j.carbpol.2018.01.072.
36 Huang F, Wei Q, Wang X & Xu W, *Polym Test*, 25 (1) (2006) 22, doi: https://doi.org/10.1016/j.polymertesting.2005.09.017.
37 Feresenbet E, Raghavan D & Holmes G, *J Adhes*, 79 (7) (2003) 643, doi: https://doi.org/10.1080/00218460309580.
38 Raharjo W W, Soenoko R, Irawan Y S & Suprapto A, *J Nat Fibers*, 15 (1) (2018) 98, doi: https://doi.org/10.1080/15440478.2017.1321512.
39 Bahrami M, Enciso B, Gaifami C M, Abenojar J & Martinez M A, *Compos Part B Eng*, 221 (2021) 109033, doi: https://doi.org/10.1016/j.compositesb.2021.109033.
40 Pandiarajan P, Kathiresan M, Baskaran P & Kanth J, *J Nat Fibers*, 19 (11) (2022) 4038, doi: https://doi.org/10.1080/15440478.2020.1852996.